Proceedings of the 4th International Conference on Mechatronics and Smart Systems
DOI: 10.54254/2755-2721/2026.34662

Design of a Lightweight Wheel Hub for New Energy Vehicles Based on ANSYS Workbench

Xuanjie Guo

Faculty of Mechanical and Energy Engineering, Beijing University of Technology, Beijing, China
23277107@emails.bjut.edu.cn

Abstract. Due to low battery energy density, new energy vehicles (NEVs) face driving range limits. Reducing wheel hub weight can lower rotational inertia and extend range. This study designs a bionic wheel hub using Vinca rosea features. Modeled in Creo and made of 6061-T6 aluminum alloy, the hub weighs 10.07 kg, achieving a 33.5% weight reduction. ANSYS simulations show that the fatigue life exceeds 1.29×10^5 cycles, which meets standard performance requirements. The first-order natural frequency also avoids main external vibrations. This design successfully balances lightweight goals and structural reliability.

Keywords: New energy vehicles, Wheel hub, Lightweight design, Finite element analysis (FEA)

1. Introduction

The automotive industry faces pressure to lower emissions and improve efficiency. Electric vehicles (EVs) are a key solution, but low battery energy density limits their driving range. Adding more batteries makes the vehicle too heavy, which hurts both handling and efficiency. Joost [1] found that a 10% weight reduction can increase an EV's driving range by about 14%. Therefore, vehicle lightweighting is a critical technical path. As an unsprung mass part, the wheel hub directly affects vehicle safety and dynamics, as noted by Yi et al. [2]. Lightening the hub reduces rotational inertia, which improves acceleration, braking, and efficiency. Thus, designing a lightweight wheel hub with high strength is very important. This study selects a pure electric sedan as a benchmark. We use Creo to design a 19-inch bionic wheel hub based on Vinca rosea, and use ANSYS to verify its strength, fatigue life, and vibration characteristics.

2. Wheel hub design

Modern wheel hub design needs to balance personalized styling and lightweight construction to improve product competitiveness.

2.1. Aesthetic design and modeling of the wheel hub

This study adopts a classic five-spoke topology as the main framework to simplify mechanical load paths. The styling draws from the natural geometry of Vinca rosea (periwinkle) petals (see Figure

© 2026 The Authors. This is an open access article distributed under the terms of the Creative Commons Attribution License 4.0 (https://creativecommons.org/licenses/by/4.0/).

DOI: 10.54254/2755-2721/2026.34662

1a). Biomorphic curved lines replace traditional straight lines to distribute mechanical loads evenly and reduce stress concentration under complex loading conditions [3, 4].

As shown in Figure 1b, the hub uses five sets of branched spokes that radiate from the center bore, mimicking a blooming petal. To cut weight, a deep reduction treatment was applied to the middle part of each spoke. This lowers the unsprung mass significantly. Meanwhile, rounded surface transitions at the edges ensure structural stiffness and a streamlined appearance. This design successfully cuts rotational inertia while maintaining high performance.



(a) Original Vinca rosea prototype (b) 3D styling design of the wheel hub

Figure 1. Wheel hub design

2.2. Wheel hub specifications and parameter design

Wheel hub parameters depend on vehicle performance, tire compatibility, and standards [5]. This design uses a pure electric sedan as a benchmark and follows the GB/T 3487-2024 standard.

To match the original chassis, the design uses the factory specifications: a 19-inch nominal diameter and an 8.5J nominal width. The rim adopts a 5° drop-center structure and a J-type rim flange to withstand lateral loads. Table 1 summarizes the specific parameters.

Table 1. Design parameters of the wheel hub

Parameter	Value
Nominal rim diameter (in)	19
Nominal rim width	8.5J
PCD (mm)	5×120
Center bore diameter (mm)	71.5
Offset	ET43
Bolt specification	M14×1.5
Tire specification	245/45 R19

2.3. Material selection for the wheel hub

Automotive wheel hubs primarily utilize cast aluminum alloys like A356.2 or forged aluminum alloys like 6061-T6 [6]. Compared with traditional casting, 6061-T6 forged aluminum offers superior mechanical properties, particularly a higher yield strength of up to 265 MPa and excellent fatigue resistance [7]. These advantages allow for thinner structural walls without sacrificing safety, providing a 20% to 30% weight reduction potential. Therefore, this study selects 6061-T6 forged aluminum alloy for the wheel hub design.

DOI: 10.54254/2755-2721/2026.34662

3. Finite element analysis

This study uses ANSYS Workbench to verify the wheel hub model. The Static Structural module simulates stress distribution under bending and impact conditions. The Fatigue Tool predicts the fatigue life from the material's S-N curve. Lockett et al. [8] noted that Finite Element Analysis (FEA) is a primary technique to evaluate structural behavior using virtual models. It helps find potential failure points before production to reduce costs.

3.1. Material properties

Defining material properties is the first step in FEA. 6061-T6 aluminum alloy is selected because it is widely used in lightweight automotive parts [9]. The material parameters are set as follows: density ρ = 2700 kg/m^3, elastic modulus E = 68.9 GPa, Poisson's ratio μ = 0.33, and yield strength σ = 275 MPa. These parameters are assigned to the wheel hub body. The S-N fatigue curve was then built from the material's ultimate tensile strength.

3.2. Meshing

Following the methods of similar hubs [10], high-order tetrahedral elements are applied to the complex hub surfaces. The ANSYS Meshing module partitions the model. To balance accuracy and speed, a global mesh size of 8 mm is selected. The final model contains 477,152 nodes and 284,766 elements. The meshing result is shown in Figure 2.



Figure 2. Schematic diagram of meshing

3.3. Static radial analysis and simulation

3.3.1. Calculation of radial load

When a vehicle travels in a straight line at a constant speed, the wheel hub mainly carries the vertical load from the body mass. This case is treated as a static condition based on the GB/T 5334-2021 standard. The static load per wheel (F_r) comes from the full-load mass of the vehicle (2630 kg):

$$F_v = \frac{(m \times g)}{4} \tag{1}$$

DOI: 10.54254/2755-2721/2026.34662

With g = 9.8 m/s^2, F_r is approximately 6443.5 N. To account for road impacts and safety margins, an enhancement factor K = 2.5 is introduced. The final radial force for simulation is $F = K \times F_r \approx 16108.8N$.

3.3.2. Boundary condition settings

The boundary conditions are set as follows. The rear surfaces of the five bolt holes and the flange contact surface are fixed to restrict all degrees of freedom. A radial force of F_r = 16108.8 N is applied upward to the inner wall of the center bore. A tire pressure of 0.3 MPa is applied to the inner surface of the rim. Standard gravity is also enabled. The constraints and loading are shown in Figure 3.



Figure 3. Schematic diagram of constraints and loading for radial static stress analysis

3.3.3. Results analysis and evaluation

In this study, the mechanical response of the wheel hub under typical operating conditions was systematically evaluated. Figure 4 shows the distributions of equivalent stress and total deformation.

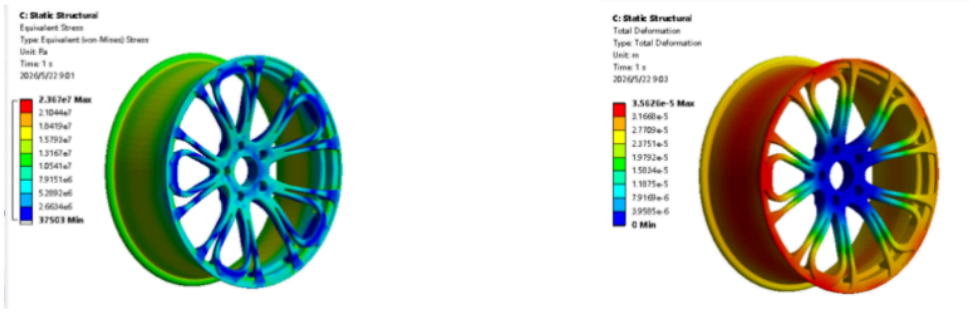

(a) Equivalent Stress Cloud Map (b) Total Deformation Cloud Map

Figure 4. Cloud maps of wheel hub radial static analysis

The simulation results show that the maximum equivalent stress is 23.67 MPa. High-stress areas appear at the fillets between the spokes and the rim, and around the bolt holes. This value is far below the yield strength of 6061-T6 (275 MPa), indicating a large safety margin. The maximum total deformation is 0.0356 mm, which shows high structural stiffness. Therefore, the static mechanical indicators meet the design safety standards.

DOI: 10.54254/2755-2721/2026.34662

3.4. Bending load simulation

3.4.1. Bending moment calculation and boundary conditions

Based on the GB/T 5334-2021 standard, this study conducts a static bending stress analysis to simulate the lateral moment during cornering. The bending moment M is calculated by formula (2). The lateral friction coefficient μ is 0.7. For the 245/45 R19 tire, the static load radius R is 0.334 m, the offset d is 0.043 m, and the reinforcement factor S is 1.6.

$$M = (\mu \cdot R + d) \cdot F_v \cdot S \tag{2}$$

The Calculated bending moment is $M \approx 2854.7N \cdot m$. To simulate this moment, the Remote Force method is used. An eccentric force F is applied at the end of a loading arm with a distance$L$of 500 mm (0.5 m). Formula (3) gives the calculation:

$$F = \frac{M}{L} \tag{3}$$

The remote force is F≈5709.4 N. The boundary conditions match the actual test bench setup. The constraints and loading are shown in Figure 5.

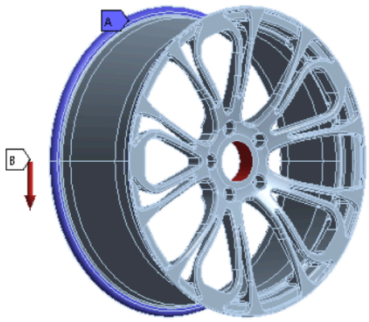

Figure 5. Schematic diagram of constraints and loading for bending static stress analysis

This study also evaluates the hub's fatigue life under cyclic loads. Su et al. [10] presented a finite element method for lightweight hubs, which provides a reference for this analysis. Based on static stress data and the S-N curve, the Fatigue Tool module calculates the fatigue life using Stress-Life Theory.

3.4.2. Results analysis and evaluation

Figure 6 shows the distributions of equivalent stress and total deformation under bending conditions.

DOI: 10.54254/2755-2721/2026.34662

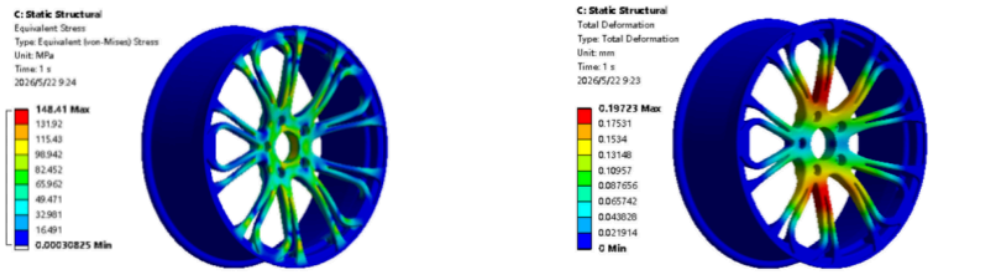

(a) Equivalent Stress Cloud Map (b) Total Deformation Cloud Map

Figure 6. Cloud maps of wheel hub bending static analysis

The simulation results show that the maximum equivalent stress is 148.41 MPa. High-stress regions concentrate at the spoke roots and around the bolt holes. This value is far below the yield strength of 6061-T6 (275 MPa), indicating a sufficient safety margin against lateral moments. The maximum total deformation is 0.193 mm, occurring near the center mounting surface. The simulation predicts a minimum fatigue life of 1.29×10^5 cycles under standard load. Figure 7 shows the distribution of fatigue life. This result satisfies the requirements of the GB/T 5334-2021 standard, confirming sound structural integrity.

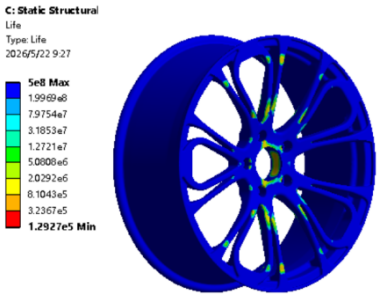

Figure 7. Fatigue Life Cloud Map

3.5. Modal analysis

Modal analysis determines the natural frequencies and mode shapes of the wheel hub. It predicts whether the hub will resonate during driving, which helps optimize structural stiffness [11]. Comparing these frequencies with external excitations helps evaluate the dynamic stability of the hub.

3.5.1. Analysis of mode shapes and natural frequencies

The first six frequencies represent rigid-body modes and are close to zero. Therefore, this paper analyzes the natural frequencies and mode shapes from the 7th to the 12th orders. The mode shapes are shown in Figure 8, and the frequencies are listed in Table 3.

DOI: 10.54254/2755-2721/2026.34662

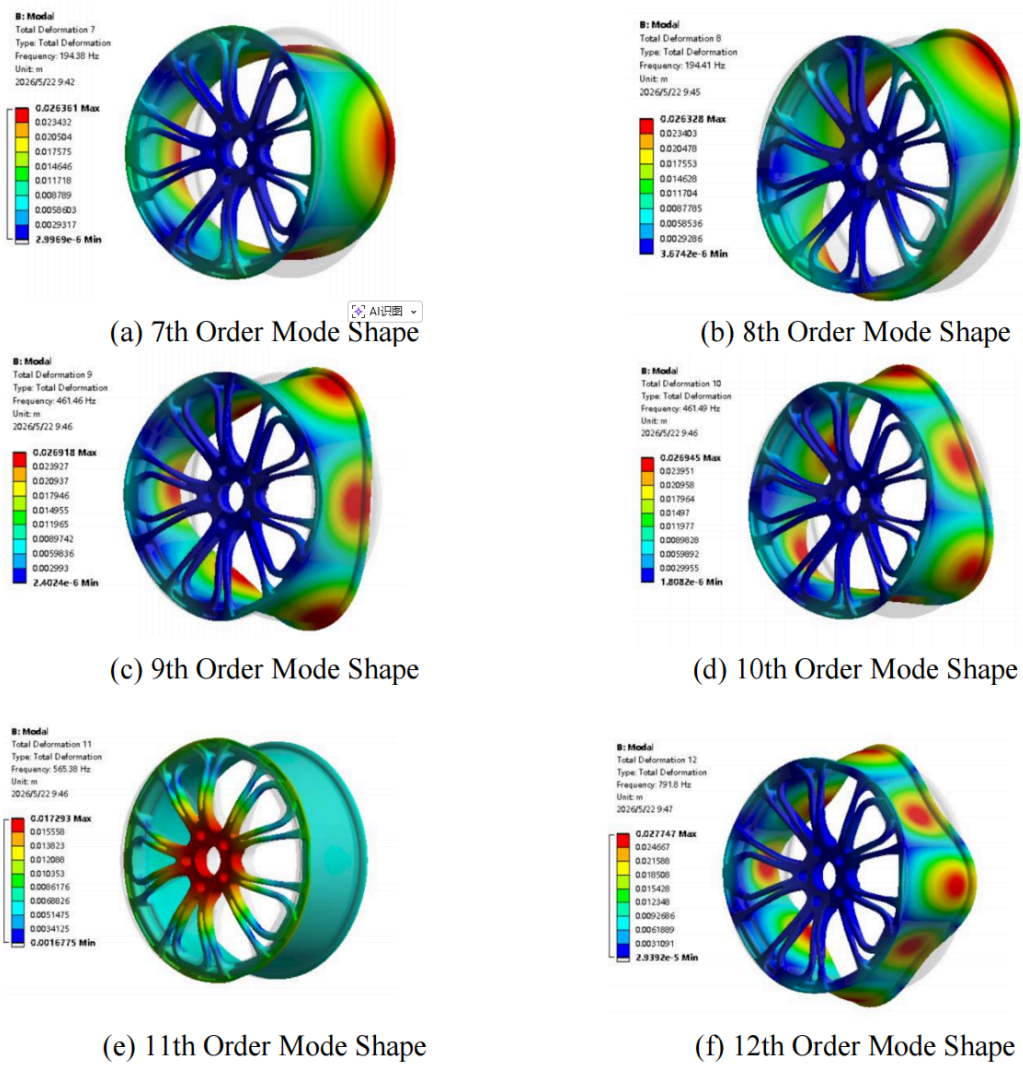

(a) 7th Order Mode Shape

(b) 8th Order Mode Shape

(c) 9th Order Mode Shape

(d) 10th Order Mode Shape

(e) 11th Order Mode Shape

(f) 12th Order Mode Shape

Figure 8. Free modal mode shapes from 7th to 12th orders

Table 3. Natural frequencies of free modes

Mode	7th Order	8th Order	9th Order	10th Order	11th Order	12th Order
Frequency (Hz)	194.38	194.41	461.46	461.49	565.38	791.8

The finite element simulation results show that the 7th/8th and 9th/10th order frequencies exhibit clear pairing characteristics, which matches the high axial symmetry of the hub structure. The 7th order is the first natural frequency of the elastic stage, with a value of 194.38 Hz. This value serves as a core indicator for evaluating the structural dynamic stability.

3.5.2. Modal analysis results and evaluation

To ensure good NVH performance, the hub's natural frequencies must avoid external excitation frequencies. For low-frequency mechanical excitation, Equation (4) gives the tire imbalance frequency. Based on vehicle speed (v) and wheel rolling radius (r), this frequency is about 14.7 Hz.

DOI: 10.54254/2755-2721/2026.34662

$$f = \frac{v}{2\pi r} \tag{4}$$

Equation (5) gives the drive shaft imbalance frequency. With a final drive ratio (i_0) of 6.1, this frequency is about 83 Hz. For road irregularities, the excitation frequency range typically falls between 1 Hz and 50 Hz. At the maximum vehicle speed (u = 120 km/h), the peak road excitation frequency is about 94 Hz. All these mechanical frequencies are far below the hub's first-order elastic natural frequency (194.38 Hz), so resonance will not occur.

$$f = \frac{v \bullet i_0}{2\pi r} \tag{5}$$

Equation (6) determines the vibration frequency of the drive motor. With a rated motor speed (n = 6000 rpm) and p = 2 pole pairs, the maximum motor frequency is 200 Hz. This value is close to the 7th order frequency (194.38 Hz). However, the damping suspension system filters these motor torque fluctuations. Because 194.38 Hz avoids the frequency ranges of normal driving speeds, the wheel hub maintains good vibration resistance.

$$f = \frac{n \cdot p}{60} \tag{6}$$

In conclusion, the wheel hub design effectively avoids resonance from main external excitation sources, demonstrating excellent dynamic stability.

4. Manufacturing process selection

Hub properties and costs depend heavily on the manufacturing route. Here, 6061-T6 alloy parts are shaped using a combined "Forged Blank + Flow Forming" technique. Forging eliminates internal voids to boost mechanical performance by 30% over standard casting. The subsequent flow forming process thins out the rim area via plastic deformation, which directly aligns and refines internal grains. This structural change drives up component strength while cutting weight by 15% to 25%, blending mass-production economics with lightweight targets. Post-forming, standard T6 heat treatment tempers the material, before a final surface coating adds essential rust protection and visual finish.

5. Conclusion

This paper presents the design and simulation of a bionic 19-inch wheel hub utilizing forged 6061-T6 aluminum. Weighing 10.07 kg, the new design sheds 33.5% of the mass found in the baseline factory hub (15.15 kg), successfully trimming the unsprung weight. Load simulations verify the hub's structural integrity. Static radial testing yields a peak stress of 23.67 MPa alongside 0.0356 mm of deformation. Under alternating bending fatigue, maximum stress reaches 148.41 MPa, guaranteeing a fatigue life beyond 1.29 $\times 10^5$ cycles to clear the GB/T 5334-2021 threshold. Furthermore, free vibration analysis marks the initial elastic natural frequency at 194.38 Hz, safely clearing potential resonance from pavement or motor inputs. In brief, the hub hits its lightweight goals without sacrificing dynamic stability.

DOI: 10.54254/2755-2721/2026.34662

References

[1] Joost, W. (2015). Energy, Materials and Vehicle Weight Reduction. U.S. Department of Energy, Office of Energy Efficiency and Renewable Energy. Retrieved from http: //www.nist.gov/mml/acmd/structural_materials/upload/Joost-W-DOE-VTP-NIST-ASP-AHSS-WorkshopR03.pdf

[2] Yi, Q. P., & Tang, C. P. (2018). Environmental Impact Assessment of Magnesium Alloy Automobile Hub Based on Life Cycle Assessment. Journal of Central South University, 25(8), 1870-1878. https: //doi.org/10.1007/s11771-018-3876-7

[3] Liu, N., Zhang, T., Li, M., & Yang, S. (2024). Bionic Optimization Design and Fatigue Life Prediction of a Honeycomb-Structured Wheel Hub. Biomimetics, 9(10), 611. doi: 10.3390/biomimetics9100611.

[4] Zhou, J. F., Guo, Z. Q., Xu, S. C., et al. (2023). Bio-Inspired Lightweight and High-strength Structures and Their Bionic Applications in Energy-absorbing Structures. Journal of Mechanical Engineering, *59*(4), 80-95. doi: 10.3901/JME.2023.04.080.

[5] State Administration for Market Regulation, & Standardization Administration of China. (2024). *GB/T 3487-2024 Passenger car rim contours series* (Chinese Standard). Beijing: China Standards Press.

[6] Richconn. (2026). 6061 T6 Aluminum Alloy: Properties, Advantages, and Industrial Applications. Retrieved March 15, 2026, from https: //richconn.com/zh-CN/6061-t6-aluminum/

[7] Aluminum Alloy Wheel Hub Network. (2026). A Brief Discussion on the Pros and Cons of Forging and Casting Processes for Aluminum Alloy and Magnesium Alloy Wheel Hubs. Retrieved March 18, 2026, from http: //alwheel.com.cn/technology/2790/

[8] Lockett, J., Fahad, M., Awan, A. W., & Islam, S. (2025). A Digital Testing Framework for Design Improvements of Three-piece Alloy Wheels Through Finite Element Analysis. Applied Sciences, 15(21), 11654. https: //doi.org/10.3390/app152111654.

[9] Hirsch, J. (2014). Recent Development in Aluminium Alloys for Automotive Application. Transactions of Nonferrous Metals Society of China, 24(7), 1995-2002. doi: 10.1016/S1003-6326(14)63319-5

[10] Su, Y., Li, J., Sun, Y., & Wang, Y. (2017). Modeling and Optimization for Lightweight Design of Aluminum Alloy Wheel Hub. Key Engineering Materials, 723, 322-327. doi: 10.4028/www.scientific.net/KEM.723.322

[11] Topaç, M. M., Ercan, S., & Kuralay, N. S. (2012). Fatigue Life Prediction of a Heavy Vehicle Steel Wheel under Radial Loads by Using Finite Element Analysis. Engineering Failure Analysis, 20, 67-79. doi: 10.1016/j.engfailanal.2011.10.007